# Molecular Theory for the Viscoelasticity of Compatible Polymer Mixtures. 1. A Tube Model Approach

**Chang Dae Han* and Jin Kon Kim**

*Department of Chemical Engineering and Polymer Research Institute, Polytechnic University, Brooklyn, New York 11201.* *Received November 30, 1987; Revised Manuscript Received September 13, 1988*

ABSTRACT: A molecular theory is developed to predict the linear viscoelastic properties of binary mixtures of compatible polymers, using the concept of the tube model of Doi and Edwards. In the development of the theory, it is assumed that each primitive chain reptates in a respective tube but that molecular interactions between the two chemically *dissimilar* primitive chains take place under the influence of an external potential. The external potential is assumed to be dependent upon the interaction parameter of the constituent components. In predicting the linear viscoelastic behavior of compatible polymer mixtures, a 3.4-power blending law is used for the relaxation modulus of the blend, $G_b(t) = [w_1G_1(t)^{1/3.4} + w_2G_2(t)^{1/3.4}]^{3.4}$, where $w_1$ and $w_2$ are the weight fractions and $G_1$ and $G_2$ are the relaxation moduli of the constituent components. Expressions are derived for zero-shear viscosity, $\eta_{0b}$, and steady-state compliance, $J_{eb}^0$, of the mixtures. The present theory predicts the following: (1) When the viscosity ratio $\eta_{01}/\eta_{02}$ of the constitutive components is much greater than 1, the log $\eta_{0b}$ versus blend composition curves show *negative* deviations from linearity for $\chi < 0$ and *positive* deviations for $\chi \approx 0$. (2) When the $\eta_{01}/\eta_{02}$ ratio is close to 1, the value of log $\eta_{0b}$ has a minimum at a certain blend composition for $\chi < 0$. (3) The value of $J_{eb}^0$ depends on both the viscosity ratio $\eta_{01}/\eta_{02}$ and the plateau modulus ratio $G_{N1}^0/G_{N2}^0$ of the constituent components, and the value of $J_{eb}^0$ may have a maximum at a certain blend composition *only* over certain ranges of $\eta_{01}/\eta_{02}$ and $G_{N1}^0/G_{N2}^0$. The predicted behavior of log $\eta_{0b}$ versus blend composition is found to be in agreement with experimental data for blends of poly(methyl methacrylate) (PMMA) and poly(vinylidene fluoride) (PVDF) and blends of PMMA and poly(styrene-*co*-acrylonitrile) (PSAN). Also derived are expressions for the dynamic storage and loss moduli, $G_b'(\omega)$ and $G_b''(\omega)$, for binary mixtures of compatible polymers. The theoretically predicted behavior of logarithmic plots of $G_b'$ versus $G_b''$ for various blend compositions is found to be in agreement with experimental data for the PMMA/PVDF blend system.

## 1. Introduction

Broadly classified, there are two types of polymer blends: heterogeneous (i.e., immiscible or incompatible) blends and homogeneous (i.e., miscible or compatible) blends. Due to their two-phase or multiphase nature, in general the viscoelastic behavior of heterogeneous polymer blends is not amenable to molecular theories, and therefore the subject has been approached from a phenomenological point of view. During the past 2 decades, numerous experimental studies have been reported on the viscoelastic behavior of heterogeneous polymer blends in the molten state. For a summary of the subject, the readers are referred to a recent monograph by Han.[1]

Dating back to the 1960s, numerous investigators[2-11] have reported on the viscoelastic behavior of binary blends of monodisperse homopolymers having *identical* chemical structure. Apparently, such effort was motivated by the desire to help understand the effect of polydispersity on the viscoelastic behavior of polymer systems. Some investigators[2-6] developed empirical or semiempirical formulas to correlate, while others[7-11] took theoretical approaches to predict, with varying degrees of success, the linear viscoelastic properties, namely, zero-shear viscosity and/or steady-state compliance of binary blends. It should be mentioned that in these efforts the chemical structure of the constituent components of the blend was identical, and thus the question of the extent of compatibility between the constituent components was not addressed.

On the other hand, when analyzing the viscoelastic data of polymer blends with *dissimilar* chemical structure, one must ask whether or not the blends under consideration are compatible. Strangely enough, there are relatively few experimental studies reported on the viscoelastic behavior of compatible polymer blends in the molten state.[12-16] One of the reasons for this may be due to the fact that there are only a few compatible polymer blend systems that have enjoyed commercial success, although in recent years an increasingly large number of compatible polymer systems have been reported.[17,18]

In 1972, Prest and Porter[12] reported on both the steady and oscillatory shearing flow properties of compatible blends of polystyrene (PS) and poly(2,6-dimethyl-1,4-phenylene oxide) (PPO) in the molten state. However, apparently due to the highly viscous nature of PPO and the thermal instability of both components, their measurements were limited to blend compositions containing 50 wt % and less of PPO. Therefore, it is not possible for one to determine the complete composition dependence of the viscoelastic properties of the blend system. Note that the compatibility of the PS/PPO blend system has been investigated extensively by several research groups.[19-23] Also, the PS/PPO blend system is one of the few compatible polymer blend systems that have enjoyed great commercial success.

In 1984, Chuang and Han[13] reported on both the steady and oscillatory shearing flow properties of blends of poly(methyl methacrylate) (PMMA) and poly(vinylidene fluoride) (PVDF) in the molten state at 210, 220, and 230 °C, over the entire range of blend compositions. They observed that the zero-shear viscosity for the blends, $\eta_{0b}$, has a *minimum* value at a certain blend composition for temperatures of 210, 220, and 230 °C, but it increases monotonically with blend composition at temperatures of 190 and 200 °C, exhibiting *negative* deviations from linearity.[24] Very recently, Wu[25] also reported *negative* deviations in a log $\eta_{0b}$ versus blend composition curve for PMMA/PVDF blends at 200 °C. Several research groups[26-30] have reported that PMMA/PVDF blends are compatible on the molecular scale.

In 1984, Aoki[14] reported on the oscillatory shearing flow properties of blends of poly(styrene-*co*-acrylonitrile) (PSAN) and poly(styrene-*co*-maleic anhydride) (PSMA) at temperatures from 140 to 240 °C, over the entire range of blend compositions. Using the relationship $\eta_0 = \lim_{\omega \to 0}$

0024-9297/89/2222-1914$01.50/0 

$G''(\omega)/\omega$, we can show that Aoki's data exhibit *negative* deviations from linearity in the log $\eta_{0b}$ versus blend composition plots.[31] The compatibility of PSAN/PSMA blends has been reported by several investigators.[32-34]

More recently, Han and Yang[15] reported on both the steady and oscillatory shearing flow properties of blends of poly(styrene-*co*-acrylonitrile) (PSAN) containing 25.3 wt % acrylonitrile and poly($\epsilon$-caprolactone) (PCL) over the entire range of blend compositions at several temperatures and showed that the blend system shows *negative* deviations in the log $\eta_{0b}$ versus blend composition plot. The compatability of PSAN/PCL blends has been investigated by several research groups.[35-38] Han and Yang[39] also investigated both the steady and oscillatory shearing flow properties of blends of poly(methyl methacrylate) (PMMA) and poly(styrene-*co*-acrylonitrile) (PSAN) at various temperatures over the entire range of blend compositions. Their data show that log $\eta_{0b}$ versus blend composition curves exhibit *positive* deviations from linearity. This observation is quite opposite to that made for the PMMA/PVDF blends. Very recently, Wu[40] also reported *positive* deviations in the log $\eta_{0b}$ versus blend composition curve for PMMA/PSAN blends at 180 °C. The compatibility of PMMA/PSAN has been investigated by several research groups.[41-46]

To the best of our knowledge, there has been no molecular theory reported on the prediction of the viscoelastic behavior of compatible polymer mixtures. In this paper we will report on our recent development of a molecular theory for the viscoelasticity of compatible polymer mixtures in the molten state.

## 2. Theory

In this section, using the concept of the tube model of Doi and Edwards,[47] we will develop a molecular theory which predicts the linear viscoelastic behavior of compatible polymer mixtures. For this, we will assume that two primitive chains with *dissimilar* chemical structure interact in an external potential and that the relaxation modulus $G_b(t)$ of a blend is described by the 3.4-power blending law. Under these assumptions, we will derive expressions for the zero-shear viscosity $\eta_{0b}$, dynamic storage and loss moduli $G_b'(\omega)$ and $G_b''(\omega)$, and the steady-state compliance $J_{eb}^0$ for binary *compatible* blends of flexible, linear *monodisperse* entangled polymers.

**a. Dynamics of the Primitive Chains with Intermolecular Interactions.** Let us consider two primitive chains, 1 and 2, representing a mixture of two polymers 1 and 2 with dissimilar chemical structure, which reptate in respective tubes. Following Graessley,[48] let us make the following assumptions: (1) the molecular weight $M$ of each polymer is larger than the entanglement molecular weight $M_e$; (2) each polymer is monodisperse; (3) for each chain, fluctuations in chain density along the tube are negligible; (4) for each chain, the path length is constant, and changes in occupation of path steps take place only by movements of the chain as a whole; thus a step located at position $x$ along some initial path ($0 < x < L$) will be occupied at a later time only if neither chain end has passed through it during that interval. This will be the case only if the chain has never moved farther than $x$ in one direction along the tube or $L - x$ in the other. In addition, we make the following assumptions: (1) the two tubes, after being mixed, retain their original diameters, $a_1$ and $a_2$, and number of segments, $Z_1$ and $Z_2$; (2) after the mixing, the motions of the two respective primitive chains are affected by the presence of other chains, and the interaction between chains can be represented by an external potential $U$.

Then the dynamics of the primitive chain 1, representing polymer 1, can be expressed in the form of the Smoluchowski equation:

$$\frac{\partial f_1}{\partial t} = D_1\frac{\partial^2 f_1}{\partial \xi_1^2} + \frac{\partial}{\partial \xi_1}\left(\frac{D_1}{k_BT}\frac{\partial U}{\partial \xi_1}\right)f_1 \tag{1}$$

where $f_1$ describes the probability that a segment of chain 1 starting at the origin at $t = 0$ will be found at a position $\xi_1$ at time $t$ later. $D_1$ is the curvilinear diffusion constant of chain 1, $k_B$ is the Boltzmann constant, $T$ is the absolute temperature, and $U$ is an external potential. If we assume that $\partial U/\partial \xi_1$ can be expressed in terms of the interaction parameter $\chi$ as given below

$$\frac{\partial}{\partial \xi_1}\left(\frac{U}{k_BT}\right) = -\frac{2(-\chi)\phi_2}{a_1} \tag{2}$$

where $\phi_2$ is the volume fraction of polymer 2 and $a_1$ is the tube diameter of chain 1, eq 1 may be rewritten as

$$\frac{\partial f_1}{\partial t} = D_1\frac{\partial^2 f_1}{\partial \xi_1^2} - \frac{2(-\chi)\phi_2 D_1}{a_1}\frac{\partial f_1}{\partial \xi_1} \tag{3}$$

The boundary conditions for eq 3 are

$$f_1(\xi_1,0) = \delta(\xi_1); \quad f_1(x_1,t) = f_1(x_1-L_1,t) = 0 \tag{4}$$

where $x_1$ is the position of chain 1 along some initial path ($0 < x_1 < L_1$) and $L_1$ is the contour length of chain 1. The solution of eq 3 becomes

$$f_1(\xi_1,t;x_1) = \frac{2}{L_1}\sum_{p=1}^{\infty}\sin\left(\frac{p\pi x_1}{L_1}\right)\sin\left(\frac{p\pi(x_1-\xi_1)}{L_1}\right)\times \exp[(-\chi)\phi_2\xi_1/a_1]\exp[-p^2t/\tau_{1,p}] \tag{5}$$

where

$$\tau_{1,p} = \left(\frac{L_1^2}{\pi^2 D_1}\right)\Big/\left[1+\left(\frac{(-\chi)\phi_2 Z_1}{p\pi}\right)^2\right] \tag{6}$$

$Z_1$ is the number of segments in primitive chain 1.

The fraction of all steps initially located at $x_1$, which are still occupied after time $t$, can be obtained by integrating eq 5, yielding

$$F_1(x_1,t) = \int_{x_1-L_1}^{x_1} f_1(\xi_1,t;x_1)\,d\xi_1 = \frac{2}{\pi}\sum_{p=1}^{\infty}\frac{1}{p}\sin\left(\frac{p\pi x_1}{L_1}\right)\exp\left[\frac{(-\chi)\phi_2 x_1}{a_1}\right]\times \exp\left[-\frac{p^2t}{\tau_{1,p}}\right]\left[\frac{1-(-1)^p\exp[-(-\chi)\phi_2 Z_1]}{1+[(-\chi)\phi_2 Z_1/p\pi]^2}\right] \tag{7}$$

Now the fraction of segments in chain 1 at time $t$, which are still in tube 1 defined at time $t = 0$ (the original tube), can be obtained by integrating eq 7, yielding

$$F_1(t) = \frac{1}{L_1}\int_0^{L_1}F_1(x_1,t)\,dx_1 = \frac{4}{\pi^2}\sum_{p=1}^{\infty}\frac{H_{1,p}}{p^2}\exp(-p^2t/\tau_{1,p}) \tag{8}$$

where $\tau_{1,p}$ is defined by eq 6 and $H_{1,p}$ is given by

$$H_{1,p} = [1-(-1)^p\cosh[(-\chi)\phi_2 Z_1]]/[1+[(-\chi)\phi_2 Z_1/p\pi]^2]^2 \tag{9}$$

Similarly, the dynamics for chain 2 representing polymer 2 can be expressed as

$$F_2(t) = \frac{4}{\pi^2}\sum_{p=1}^{\infty}\frac{H_{2,p}}{p^2}\exp(-p^2t/\tau_{2,p}) \tag{10}$$

where

$$\tau_{2,p} = \left(\frac{L_2^2}{\pi^2 D_2}\right) \Big/ \left[1 + \left(\frac{(-\chi)\phi_1 Z_2}{p\pi}\right)^2\right] \quad (11)$$

$$H_{2,p} = [1 - (-1)^p \cosh [(-\chi)\phi_1 Z_2]]/[1 + [(-\chi)\phi_1 Z_2/p\pi]^2]^2 \quad (12)$$

$L_2$ is the contour length and $Z_2$ the number of segments in chain 2.

Let us assume that the relaxation modulus $G_b(t)$ for a binary polymer mixture is given by a 3.4-power blending law

$$G_b(t) = [w_1 G_1(t)^{1/3.4} + w_2 G_2(t)^{1/3.4}]^{3.4} \quad (13)$$

where $w_1$ and $w_2$ are the weight fractions and $G_1(t)$ and $G_2(t)$ are the relaxation moduli for polymers 1 and 2, respectively. Equation 13 can be rewritten in terms of the functions $F_1(t)$ and $F_2(t)$, defined by eq 8 and 10, respectively, as

$$G_b(t) = [w_1[G_{N1}^0 F_1(t)]^{1/3.4} + w_2[G_{N2}^0 F_2(t)]^{1/3.4}]^{3.4} \quad (14)$$

where $G_{N1}^0$ and $G_{N2}^0$ are the plateau moduli of polymers 1 and 2, respectively. From eq 8, 10, and 14 we have

$$G_b(t) = \frac{4}{\pi^2}\left[ w_1\left[ G_{N1}^0 \sum_{p=1}^{\infty} \frac{H_{1,p}}{p^2} \exp(-p^2 t/\tau_{1,p})\right]^{1/3.4} + w_2\left[ G_{N2}^0 \sum_{p=1}^{\infty} \frac{H_{2,p}}{p^2} \exp(-p^2 t/\tau_{2,p})\right]^{1/3.4}\right]^{3.4} \quad (15)$$

**b. Zero-Shear Viscosity $\eta_{0b}$ for Compatible Polymer Blends.** We can now calculate the zero-shear viscosity $\eta_{0b}$ for a binary blend from

$$\eta_{0b} = \int_0^{\infty} G_b(t)\, dt = \frac{4}{\pi^2}\int_0^{\infty}\left[\sum_{i=1}^{2} w_i\left[ G_{Ni}^0 \sum_{p=1}^{\infty} \frac{H_{i,p}}{p^2} \exp(-p^2 t/\tau_{i,p})\right]^{1/3.4}\right]^{3.4} dt \quad (16)$$

Because analytical integration of eq 16 is not possible, the following *approximate* expression is obtained for $\eta_{0b}$ (see Appendix):

$$\eta_{0b} = \frac{48}{\pi^4}\left[\sum_{i=1}^{2} w_i\left[ \eta_{0i} \sum_{p=1}^{\infty} \frac{1}{p^4} \times \frac{(1 - (-1)^p \cosh [(-\chi)\phi_i^* Z_i])}{(1 + [(-\chi)\phi_i^* Z_i/p\pi]^2)^3}\right]^{1/3.4}\right]^{3.4} \quad (17)$$

where $\phi_1^* = \phi_2$ and $\phi_2^* = \phi_1$.

**c. Steady-State Compliance $J_{eb}^0$ for Compatible Polymer Blends.** We can calculate the steady-state compliance $J_{eb}^0$ from

$$J_{eb}^0 = \int_0^{\infty} t G_b(t)\, dt \Big/ \left[\int_0^{\infty} G_b(t)\, dt\right]^2 \quad (18)$$

From eq 15 and 18 we obtain the following *approximate* expression for $J_{eb}^0$ (see Appendix):

$$J_{eb}^0 = \frac{576}{\pi^6 \eta_{0b}^2}\left[\sum_{i=1}^{2} w_i\left[ \frac{\eta_{0i}^2}{G_{Ni}^0} \sum_{p=1}^{\infty} \frac{1}{p^6} \times \frac{(1 - (-1)^p \cosh [(-\chi)\phi_i^* Z_i])}{(1 + [(-\chi)\phi_i^* Z_i/p\pi]^2)^4}\right]^{1/3.4}\right]^{3.4} \quad (19)$$

It can be shown that for $\chi = 0$ eq 19 reduces to

$$J_{eb}^0 = \frac{6}{5}\frac{1}{G_{N2}^0}\left[\frac{(1 - w_2)(r_v^2/r_G)^{1/3.4} + w_2}{[(1 - w_2) r_v^{1/3.4} + w_2]^2}\right]^{3.4} \quad (20)$$

where

$$r_v = \eta_{01}/\eta_{02}; \quad r_G = G_{N1}^0/G_{N2}^0 \quad (21)$$

Note that for binary compatible blends in general, the plateau moduli of the constituent components, $G_{N1}^0$ and $G_{N2}^0$, have different values. However, for binary blends with *identical* chemical structure, we have $r = 1/r_v^{1/3.4} = M_2/M_1$, where $M_1$ and $M_2$ are the molecular weights of the constituent components and $G_N^0 = G_{N1}^0 = G_{N2}^0$; thus eq 20 reduces to

$$J_{eb}^0 = \frac{6}{5}\frac{1}{G_N^0}\left[\frac{1 - w_2 + r^2 w_2}{(1 - w_2 + r w_2)^2}\right]^{3.4} \quad (22)$$

**d. Dynamic Moduli $G_b'(\omega)$ and $G_b''(\omega)$ for Compatible Polymer Blends.** With the aid of eq 15, *approximate* expressions for the dynamic storage modulus $G_b'(\omega)$ and dynamic loss modulus $G_b''(\omega)$ are obtained as follows (see Appendix):

$$G_b'(\omega) = \frac{4}{\pi^2}\left[\sum_{i=1}^{2} w_i\left[ G_{Ni}^0 \sum_{p=1}^{\infty} \frac{H_{i,p}}{p^2} \frac{(\omega\tau_{i,p}/p^2)^2}{1 + (\omega\tau_{i,p}/p^2)^2}\right]^{1/3.4}\right]^{3.4} \quad (23)$$

$$G_b''(\omega) = \frac{4}{\pi^2}\left[\sum_{i=1}^{2} w_i\left[ G_{Ni}^0 \sum_{p=1}^{\infty} \frac{H_{i,p}}{p^2} \frac{\omega\tau_{i,p}/p^2}{1 + (\omega\tau_{i,p}/p^2)^2}\right]^{1/3.4}\right]^{3.4} \quad (24)$$

where $\tau_{1,p}$ and $\tau_{2,p}$ are defined by eq 6 and 11, respectively, and $H_{1,p}$ and $H_{2,p}$ are defined by eq 9 and 12, respectively.

Note that $\eta_{0b}$ (see eq 17) can be derived from eq 24 and $J_{eb}^0$ (see eq 19) from eq 23 and 24 with the aid of the following relationship:

$$J_{eb}^0 = \lim_{\omega \to 0} \frac{G_b'(\omega)}{[G_b''(\omega)]^2} \quad (25)$$

## 3. Predictions of Theory

We will now show predictions of the theory developed above. For this, let us consider blends of PMMA and PVDF and designate PMMA as component 1 and PVDF as component 2. To be consistent with the assumptions made in the theory presented above, let us assume that both PMMA and PVDF are monodisperse, with molecular weights $M_1 = 7.92 \times 10^4$ and $M_2 = 1.45 \times 10^5$. It should be mentioned that these values represent the weight-average molecular weights ($\bar{M}_w$) of the polydisperse PMMA and PVDF used in the viscosity measurements reported by Chuang and Han.[13] Using the plateau modulus $G_{N1}^0 = 6.0 \times 10^5$ Pa for PMMA and $G_{N2}^0 = 4.5 \times 10^5$ Pa for PVDF as determined in our laboratory,[49] we calculated the number of segments to be $Z_1 = 13.8$ for PMMA and $Z_2 = 12.2$ for PVDF, using the expression[48]

$$Z_i = \frac{5}{4}\frac{M_i}{M_{ei}} \quad (26)$$

where $M_i$ ($i = 1, 2$) are the molecular weights and $M_{ei}$ ($i = 1, 2$) are the entanglement molecular weights of the constituent components. The entanglement molecular weight is determined to be $M_{e1} = 7.1 \times 10^3$ for PMMA and $M_{e2} = 1.5 \times 10^4$ for PVDF, using the expression $M_{ei} =$

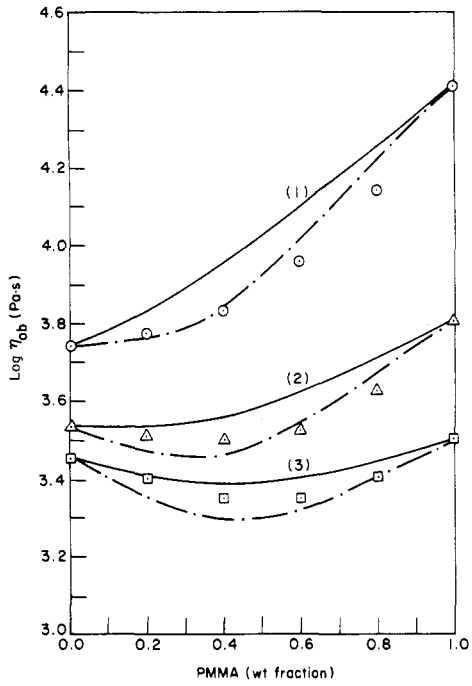


**Figure 1.** Theoretically predicted dependence of log $\eta_{0b}$ on blend composition for the PMMA/PVDF blends at various temperatures. Curve 1 at 200 °C; curve 2 at 220 °C; and curve 3 at 230 °C. Here, the solid curve was obtained with $\chi = -0.3$ and the broken curve with $\chi = -0.5$. Symbols for the data points are as follows: (⊙) $T$ = 200 °C and $\eta_0$(PMMA)/$\eta_0$(PVDF) = 4.66; (▲) $T$ = 220 °C and $\eta_0$(PMMA)/$\eta_0$(PVDF) = 1.87; (⊡) $T$ = 230 °C and $\eta_0$(PMMA)/$\eta_0$(PVDF) = 1.10.

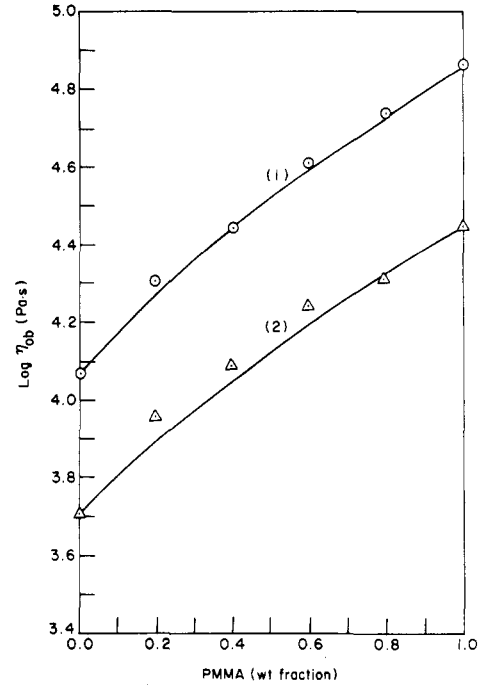


**Figure 2.** Theoretically predicted dependence of log $\eta_{0b}$ on blend composition for the PMMA/PSAN blends at various temperatures. Curve 1 at 200 °C and curve 2 at 210 °C. Here, $\chi = -0.01$ was used in the computation. Symbols for the data points are as follows: (⊙) $T$ = 200 °C and $\eta_0$(PMMA)/$\eta_0$(PSAN) = 6.15; (▲) $T$ = 210 °C and $\eta_0$(PMMA)/$\eta_0$(PSAN) = 5.5.

$\rho_i RT/G_{Ni}^0$ ($i$ = 1, 2), where $\rho$ is the density, $R$ is the universal gas constant, and $T$ is the absolute temperature.

Negative values of the interaction parameter $\chi$ for PMMA/PVDF mixtures are reported in the literature.[28,50] Using the values of $Z_1$ and $Z_2$ estimated above and the values of $-\chi = 0.3$ and 0.5, respectively, we have calculated $\eta_{0b}$ for the PMMA/PVDF blends at different temperatures using eq 17, and the results are given in Figure 1. It can be seen in Figure 1 that the theory predicts the essential features of the experimental results, namely, log $\eta_{0b}$ has a minimum value at a certain blend composition at 230 °C and shows *negative* deviations from linearity at 200 °C. Note that the theoretical predictions in Figure 1 are based on the assumption that both PMMA and PVDF are monodisperse, while they are actually polydisperse, and that a constant value of $\chi$ was assumed over the range of temperature considered. For blends exhibiting an LCST, it is expected that the value of $-\chi$ will increase with decreasing temperature. At present, there is no experimental data available that describe the dependence of $\chi$ on temperature for the PMMA/PVDF blend system. It is gratifying to observe in Figure 1 that at 230 °C log $\eta_{0b}$ has a minimum value at a certain blend composition when the viscosity ratio, $\eta_{01}$(PMMA)/$\eta_{02}$(PVDF), is close to 1 and that at 200 °C it increases monotonically with increasing weight fraction of PMMA, exhibiting negative deviations, as the value of $\eta_{01}/\eta_{02}$ becomes much greater than 1.

Figure 2 shows theoretical predictions of log $\eta_{0b}$ versus blend composition curves for the PMMA/PSAN blend system, obtained by using the value of $-\chi = 0.01$ reported by Schmitt and co-workers.[51] In the theoretical predictions the following numerical values were used for the various molecular parameters:[49] (1) $M_1 = 1.05 \times 10^5$ for PMMA and $M_2 = 1.50 \times 10^5$ for PSAN; (2) $Z_1 = 18.8$ for PMMA and $Z_2 = 10.3$ for PSAN; and (3) $G_{N1}^0 = 6.0 \times 10^5$ Pa for PMMA and $G_{N2}^0 = 2.28 \times 10^5$ Pa for PSAN. It is of interest to observe in Figure 2 that the theory predicts *positive* deviations from linearity in the log $\eta_{0b}$ versus blend composition plot.

It can then be concluded that the shape of log $\eta_{0b}$ versus blend composition curves depends very much on the values of the interaction parameter $\chi$ between the constituent components in a given blend system, i.e., the larger the value of $-\chi$, the greater the extent of *negative* deviations in the log $\eta_{0b}$ versus blend composition plots. Specifically, the negative deviations observed in the log $\eta_{0b}$ versus blend composition curves for the PMMA/PVDF blends are attributed to the rather large negative values of the interaction parameter $\chi$ between the PMMA and PVDF. The positive deviations observed in the log $\eta_{0b}$ versus blend composition curves for the PMMA/PSAN blends are attributable to the nearly zero value of $\chi$ between the PMMA and PSAN.

Han and co-workers[13,15,52-56] have shown that logarithmic plots of $G'$ versus $G''$ are very useful in investigations of linear viscoelastic properties of flexible linear homopolymers and their blends. It has been found that log $G'$ versus log $G''$ plots are *virtually* independent of temperature and molecular weight for monodisperse polymers and that the slope of log $G'$ versus log $G''$ plots decreases from 2 in the terminal region to a lower value in the linear region. In their recent paper, Chuang and Han[13] have presented log $G'$ versus log $G''$ plots for PMMA/PVDF blends, as reproduced in Figure 3. It can be seen in Figure 3 that for a fixed value of $G''$ values of $G'$ of the blends lie between those of the constituent components. Figure 4 gives theoretically predicted plots of dynamic storage modulus $G_b'$ versus dynamic loss modulus $G_b''$ on logarithmic coordinates for the PMMA/PVDF blends. Note that the plots were obtained by using eq 23 and 24 and the same numerical values of the parameters used to generate the results given in Figure 1. A comparison between Figure 3 and Figure 4 indicates that at fixed values of $G_b''$ the values of $G_b'$ are smaller than those measured experimentally; however, the dependencies predicted for

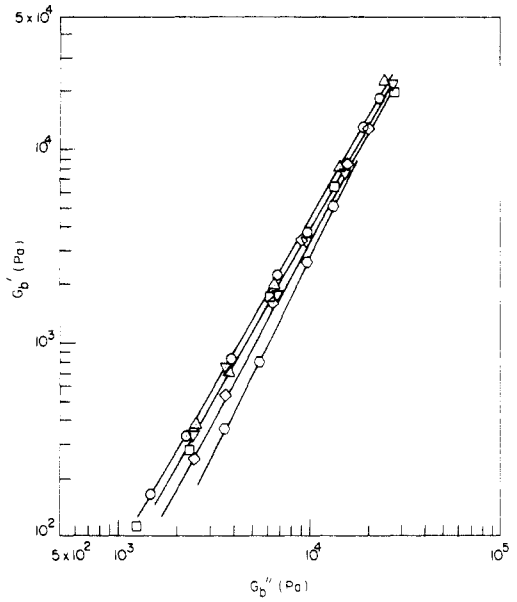


**Figure 3.** log $G_b'$ versus log $G_b''$ for binary blends of PMMA and PVDF at 230 °C:[13] (⊙) PVDF; (⊙) PMMA; (▲) PVDF/PMMA = 80/20; (⊡) PVDF/PMMA = 60/40; (▼) PVDF/PMMA = 40/60; (◇) PVDF/PMMA = 20/80.

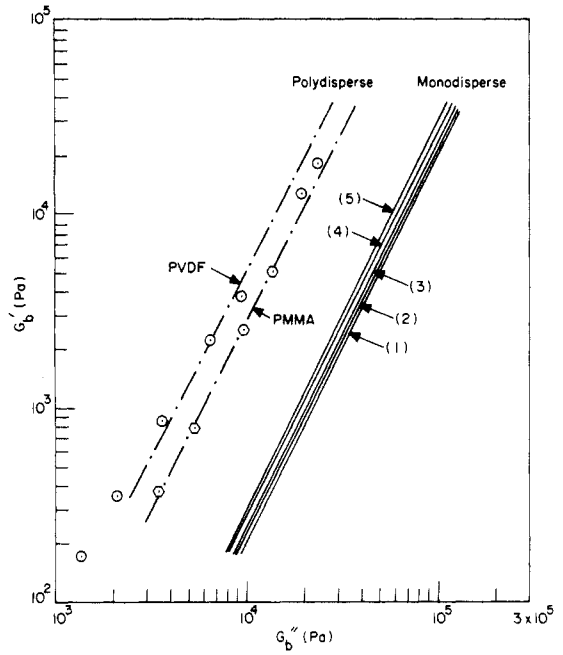


**Figure 4.** Theoretically predicted log $G_b'$ versus log $G_b''$ plots for PMMA/PVDF blends at 230 °C: (1) PMMA; (2) PMMA/PVDF = 80/20; (3) PMMA/PVDF = 60/40; (4) PMMA/PVDF = 20/80; (5) PVDF. Here, $\chi = -0.3$ was used in the computation. The broken curves (– · –) were obtained by using eq 28 for polydisperse PMMA and PVDF. Symbols for the data points are as follows: (⊙) PVDF; (⊙) PMMA.

log $G_b'$ versus log $G_b''$ plots on blend composition are consistent with those observed experimentally.

Note, however, that eq 23 and 24 were derived under the assumption that the constituent components are monodisperse. Earlier, Han and Jhon[55] predicted that for *monodisperse* linear entangled homopolymers log $G'$ versus log $G''$ plots in the terminal region can be described by the expression[57]

$$\log G' = 2 \log G'' + \log (6/5G_N^0) \tag{27}$$

Very recently, we developed a theory,[58] which predicts the effect of polydispersity on log $G_b'$ versus log $G_b''$ plots for

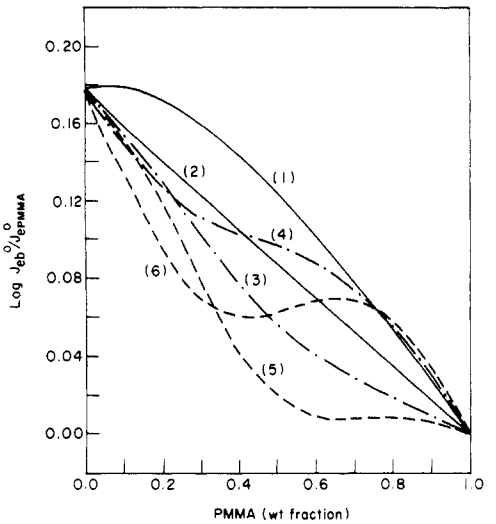


**Figure 5.** Theoretically predicted dependence of log ($J_{eb}^0/J_{ePMMA}^0$) on blend composition for the PMMA/PVDF blends: curve 1 for $\eta_{01}/\eta_{02} = 1.11$ and $\chi = 0$; curve 2 for $\eta_{01}/\eta_{02} = 4.66$ and $\chi = 0$; curve 3 for $\eta_{01}/\eta_{02} = 1.11$ and $\chi = -0.3$; curve 4 for $\eta_{01}/\eta_{02} = 4.66$ and $\chi = -0.3$; curve 5 for $\eta_{01}/\eta_{02} = 1.11$ and $\chi = -0.5$; and curve 6 for $\eta_{01}/\eta_{02} = 4.66$ and $\chi = -0.5$.

linear entangled homopolymers in the *terminal* region as follows:

$$\log G_b' = 2 \log G_b'' + \log (6/5G_N^0) + 3.4 \log (\bar{M}_z/\bar{M}_w) \tag{28}$$

where $\bar{M}_z$ and $\bar{M}_w$ are $z$-average and weight-average molecular weights, respectively. According to eq 28, the values of $G_b'$ for a polydisperse homopolymer will be shifted upward by the amount 3.4 log ($\bar{M}_z/\bar{M}_w$) above the values of $G'$ for monodisperse polymers; thus the shift will be greater with increasing polydispersity, $\bar{M}_z/\bar{M}_w$. Now, if we include the effect of polydispersities of the PMMA ($\bar{M}_w = 7.92 \times 10^4$ and $\bar{M}_n = 3.66 \times 10^4$) and PVDF ($\bar{M}_w = 1.45 \times 10^5$ and $\bar{M}_n = 6.30 \times 10^4$) in the log $G_b'$ versus log $G_b''$ plots with an assumption of log normal distribution function, the theoretical predictions of log $G_b'$ versus log $G_b''$ plots become reasonably close to the experimental results, as shown in Figure 4.

It should be noted that the slope of the log $G_b'$ versus log $G_b''$ plots for PMMA and PVDF in Figure 4 is equal to 2, since eq 28 is valid in the terminal region (i.e., as $G_b'' \to 0$). However, *outside* the terminal region the slope of log $G_b'$ versus log $G_b''$ plots decreases from 2 with increasing polydispersity.[58] Since the polydispersity of PVDF is 2.31, whereas the polydispersity of PMMA is 2.16, the slope of log $G_b'$ versus log $G_b''$ plots for the PVDF should be smaller than that for the PMMA. This now explains why in Figure 3 the slope of the experimentally determined log $G'$ versus log $G''$ plots for pure PVDF is smaller than that for pure PMMA.

## 4. Discussion

It is a well-established fact[7,11,59] that the steady-state compliance $J_{eb}^0$ for binary polymer blends with *identical* chemical structure has a maximum value at a certain blend composition. This can be seen through eq 22, where $J_{eb}^0$ has a maximum value at the composition

$$(w_2)_c = 1/(1 + r) \tag{29}$$

where $r$ is the ratio of the component molecular weights, $M_2/M_1$.

Figure 5 gives plots of log ($J_{eb}^0/J_{ePMMA}^0$) versus blend composition for the PMMA/PVDF blends, where $J_{ePMMA}^0$ is the steady-state compliance of the PMMA. Note that

the curves in Figure 5 were obtained by using eq 19. It can be seen in Figure 5 that there is *no* maximum in $J_{eb}^0$ over the entire blend composition at 200 and 230 °C for negative values of $\chi$, but a slight maximum in $J_{eb}^0$ appears at a weight fraction of PMMA of about 0.1 at 200 °C for $\chi = 0$. Note that for the PMMA/PVDF blend system under consideration $G_{N1}^0$(PMMA) = 6.0 × 10⁵ Pa, $G_{N2}^0$(PVDF) = 4.5 × 10⁵ Pa, and $\eta_{01}$(PMMA)/$\eta_{02}$(PVDF) = 1.11 at 230 °C and 4.66 at 200 °C. Equation 19 indicates that the values of $J_{eb}^0$ depend on both the $\eta_{01}/\eta_{02}$ and $G_{N1}^0/G_{N2}^0$ ratios.

Since it is not easy to obtain an analytical expression from eq 19 for the composition at which the value of $J_{eb}^0$ is a maximum, let us consider, for the purpose of illustration, a situation where $\chi = 0$ in eq 19. It can be shown from eq 20 that $J_{eb}^0$ has a maximum value at the composition

$$(w_2)_c = \frac{r_v^{1/3.4} + (r_v^2/r_G)^{1/3.4}(r_v^{1/3.4} - 2)}{[(r_v^2/r_G)^{1/3.4} - 1](r_v^{1/3.4} - 1)} \quad (30)$$

It can be seen from eq 30 that $J_{eb}^0$ has a maximum value *only* over a limited range of $r_v$ and $r_G$. Specifically, eq 30 indicates that as $r_v \to 1$, $(w_2)_c \to \infty$, which is physically *not* possible. However, if $r_G \approx 1$ (i.e., $G_{N1}^0 \approx G_{N2}^0$ and $J_{e1}^0 \approx J_{e2}^0$), eq 30 reduces to

$$(w_2)_c = \frac{1}{1 + (1/r_v)^{1/3.4}} \quad (31)$$

indicating that $J_{eb}^0$ always has a maximum value at the composition $(w_2)_c$ defined by eq 31. Note that for compatible polymer blends with *dissimilar* chemical structure, $r_v^{1/3.4} = (\eta_{01}/\eta_{02})^{1/3.4}$ *cannot* be equated to $1/r = M_1/M_2$, since $\eta_{01} = K_1M_1^{3.4}$, $\eta_{02} = K_2M_2^{3.4}$, and $K_1$ is not equal to $K_2$. Only when $K_1 = K_2$ (i.e., for binary blends with *identical* chemical structure) does $r_v^{1/3.4} = 1/r$, and consequently eq 31 reduces to eq 29. Therefore, it can be concluded that both $r_G$ and $r_v$ play an important role in determining the blend composition at which the value of $J_{eb}^0$ is a maximum.

Note that for binary blends of monodisperse homopolymers with *identical* chemical structure log $\eta_{0b}$ varies monotonically with blend composition, exhibiting positive deviations from linearity.[60] Note that when a blend consists of two components with *identical* chemical structure, the weight-average molecular weight $\bar{M}_{wb}$ of the blend can be given by

$$\bar{M}_{wb} = w_1\bar{M}_{w1} + w_2\bar{M}_{w2} \quad (32)$$

where $w_1$ and $w_2$ are the weight fractions of components 1 and 2, respectively, and $\bar{M}_{w1}$ and $\bar{M}_{w2}$ are weight-average molecular weights of components 1 and 2, respectively. Thus, when the zero-shear viscosities, $\eta_{01}$ and $\eta_{02}$, of the constituent components follow the 3.4-power law with respect to $\bar{M}_{wi}$ ($i = 1, 2$), i.e., $\eta_{0i} \propto \bar{M}_{wi}^{3.4}$, the zero-shear viscosity of the blend, $\eta_{0b}$, can be expressed as

$$\eta_{0b} = [w_1\eta_{01}^{1/3.4} + w_2\eta_{02}^{1/3.4}]^{3.4} \quad (33)$$

It is clear from eq 33 that in *no* way can log $\eta_{0b}$ exhibit negative deviations with respect to blend composition. It should be pointed out that the use of eq 32 is not valid for blends whose constituent components have *dissimilar* chemical structure.

In the theoretical development presented above we have assumed that the relaxation modulus $G_b(t)$ of a binary blend follows the 3.4-power blending law. Admittedly, the choice of this blending law is arbitrary, and therefore other blending laws can be used. Note that a linear blending law, for instance, does not correctly predict the trend in the dependency of $\eta_{0b}$ on molecular weight, but the 3.4-power blending law does. One of the limitations of using the 3.4-power blending law is that, due to the highly nonlinear nature of its expression, eq 15 is not amenable to an analytical solution for $\eta_{0b}$. Therefore we obtained *approximate* analytical expressions for $\eta_{0b}$, $J_{eb}^0$, $G_b'(\omega)$, and $G_b''(\omega)$ (see Appendix). The obtainment of *approximate* analytical expressions has enabled us to explain under what circumstances the seemingly strange experimental observations, such as a minimum in the log $\eta_{0b}$ versus blend composition plot, can occur.

At this juncture it should be mentioned that, according to the experimental data by Masuda et al.,[61] the zero-shear viscosity $\eta_0$ of PMMA for molecular weights $M > 10^5$ follows the 3.4-power law, which is consistent *qualitatively* with the predictions of the tube model by Doi and Edwards.[47] However, the steady-state compliance $J_e^0$ of PMMA was found to increase with molecular weight even when it was as high as 3.4 × 10⁵. This seems to suggest that the elastic behavior of PMMA for $M \approx 3 \times 10^5$ is *not* consistent with the predictions of the tube model since, according to the tube model, $J_e^0$ should become independent of molecular weight for $M > M_e$. On the other hand, it has been found empirically[62] that $J_e^0$ becomes independent of molecular weight when $M > M_c'$, where the value of $M_c'$ was found to be 6–7 times that of $M_e$. According to Masuda et al.,[61] the value of $M_e$ for PMMA varies from 6.7 × 10³ to 1.3 × 10⁴, depending on its molecular weight (4.5 × 10⁴ to 3.4 × 10⁵), and Graessley[62] speculated that the value of $M_c'$ for PMMA might be greater than 1.5 × 10⁵. We believe that the tube model will predict the viscoelastic behavior of PMMA with molecular weight sufficiently high (say $M > 3 \times 10^5$). Therefore, for the PMMA with $M < M_c'$, which is the situation referred to in Figure 4, we maintain the view that the reasonable agreement observed between theoretical predictions and experimental data in the log $G'$ versus log $G''$ plots may not necessarily warrant the use of the tube model approach, at least until experimental values of $G'$ and $G''$ for *monodisperse* PMMA having the same molecular weight as that used in our theoretical investigation become available.

## 5. Concluding Remarks

We have presented a molecular theory that predicts the zero-shear viscosity $\eta_{0b}$, steady-state compliance $J_{eb}^0$, dynamic storage modulus $G_b'(\omega)$, and dynamic loss modulus $G_b''(\omega)$ for compatible polymer mixtures having dissimilar chemical structures. The theory is based on the concept of the tube model due to Doi and Edwards,[47] but never before, to the best of our knowledge, has the tube model originally developed for flexible homopolymers been extended to mixtures of two compatible polymers having *dissimilar* chemical structures. We have shown above that the interaction parameter $\chi$ plays a central role in determining the shape of the log $\eta_{0b}$ versus blend composition curve for compatible polymer mixtures. The present theory explains the physical origin of some of the linear viscoelastic properties observed experimentally in compatible polymer mixtures, namely, *negative* deviations from linearity in the log $\eta_{0b}$ versus blend composition plots for the PMMA/PVDF blends and *positive* deviations for the PMMA/PSAN blends. The present theory correctly predicts the general dependence of log $G'$ versus log $G''$ plots on blend composition for compatible polymer mixtures.

Although we feel that theoretical approach taken to determine the viscoelastic properties of compatible polymer mixtures expressed in terms of the interaction pa-

rameter $\chi$ is a step in the right direction, the good agreement observed between theory and experiment does not necessarily warrant the use of the position-independent potential function (see eq 2). In a future study, we will employ a position-dependent potential function and will also include constraint release in the tube model of Doi and Edwards, in the investigation of the viscoelastic behavior of compatible polymer mixtures.

## Appendix

When an analytical expression for the relaxation modulus $G_b(t)$ is known, the zero-shear viscosity $\eta_{0b}$ can be determined from

$$\eta_{0b} = \int_0^\infty G_b(t)\, dt \tag{A1}$$

Substitution of eq 15 into eq A1 gives

$$\eta_{0b} = \frac{4}{\pi^2}\int_0^\infty \left[ w_1 \left[ G_{N1}^0 \sum_{p=1}^\infty \frac{H_{1,p}}{p^2} \exp(-p^2 t/\tau_{1,p}) \right]^{1/3.4} + w_2 \left[ G_{N2}^0 \sum_{p=1}^\infty \frac{H_{2,p}}{p^2} \exp(-p^2 t/\tau_{2,p}) \right]^{1/3.4} \right]^{3.4} dt \tag{A2}$$

where $\tau_{1,p}$ and $\tau_{2,p}$ are defined by eq 6 and eq 11, respectively, and $H_{1,p}$ and $H_{2,p}$ are defined by eq 9 and 12, respectively. Because an analytical integration of eq A2 is not possible, the following *approximate* expression is obtained:

$$\eta_{0b} = \frac{4}{\pi^2}\left[ w_1 \left[ \int_0^\infty G_{N1}^0 \sum_{p=1}^\infty \frac{H_{1,p}}{p^2} \exp(-p^2 t/\tau_{1,p})\, dt \right]^{1/3.4} + w_2 \left[ \int_0^\infty G_{N2}^0 \sum_{p=1}^\infty \frac{H_{2,p}}{p^2} \exp(-p^2 t/\tau_{2,p})\, dt \right]^{1/3.4} \right]^{3.4} \tag{A3}$$

Now, integration of eq A3 gives eq 17. Note that in the derivation of eq 17 use is made of the relationships[63]

$$\eta_{01} = \frac{1}{12} G_{N1}^0 \frac{L_1^2}{D_1}; \quad \eta_{02} = \frac{1}{12} G_{N2}^0 \frac{L_2^2}{D_2} \tag{A4}$$

When an analytical expression for the relaxation modulus $G_b(t)$ is known, the steady-state compliance $J_{eb}^0$ can be determined from

$$J_{eb}^0 = \int_0^\infty G_b(t) t\, dt \Big/ \left[ \int_0^\infty G_b(t)\, dt \right]^2 \tag{A5}$$

Substitution of eq 15, with the aid of eq A1, into eq A5 gives

$$J_{eb}^0 = \frac{4}{\pi^2 \eta_{0b}^2} \times \int_0^\infty \left[ w_1 \left[ G_{N1}^0 \sum_{p=1}^\infty \frac{H_{1,p}}{p^2} \exp(-p^2 t/\tau_{1,p}) \right]^{1/3.4} + w_2 \left[ G_{N2}^0 \sum_{p=1}^\infty \frac{H_{2,p}}{p^2} \exp(-p^2 t/\tau_{2,p}) \right]^{1/3.4} \right]^{3.4} t\, dt \tag{A6}$$

Because analytical integration of eq A6 is not possible, the following *approximate* expression is obtained:

$$J_{eb}^0 = \frac{4}{\pi^2 \eta_{0b}^2} \times \left[ w_1 \left[ \int_0^\infty G_{N1}^0 \sum_{p=1}^\infty \frac{H_{1,p}}{p^2} \exp(-p^2 t/\tau_{1,p}) t\, dt \right]^{1/3.4} + w_2 \left[ \int_0^\infty G_{N2}^0 \sum_{p=1}^\infty \frac{H_{2,p}}{p^2} \exp(-p^2 t/\tau_{2,p}) t\, dt \right]^{1/3.4} \right]^{3.4} \tag{A7}$$

Now, integration of eq A7 gives eq 19.

The dynamic storage modulus $G_b'(\omega)$ can be obtained from

$$G_b'(\omega) = \omega \int_0^\infty G_b(t) \sin \omega t\, dt \tag{A8}$$

and the dynamic loss modulus $G_b''(\omega)$ from

$$G_b''(\omega) = \omega \int_0^\infty G_b(t) \cos \omega t\, dt \tag{A9}$$

Substitution of eq 15 into eq A8 gives

$$G_b'(\omega) = \omega \int_0^\infty \frac{4}{\pi^2} \left[ w_1 \left[ G_{N1}^0 \sum_{p=1}^\infty \frac{H_{1,p}}{p} \times \exp(-p^2 t/\tau_{1,p}) \right]^{1/3.4} + w_2 \left[ G_{N2}^0 \sum_{p=1}^\infty \frac{H_{2,p}}{p^2} \exp(-p^2 t/\tau_{2,p}) \right]^{1/3.4} \right]^{3.4} \sin \omega t\, dt \tag{A10}$$

and substitution of eq 15 into eq A9 gives

$$G_b''(\omega) = \omega \int_0^\infty \frac{4}{\pi^2} \left[ w_1 \left[ G_{N1}^0 \sum_{p=1}^\infty \frac{H_{1,p}}{p^2} \times \exp(-p^2 t/\tau_{1,p}) \right]^{1/3.4} + w_2 \left[ G_{N2}^0 \sum_{p=1}^\infty \frac{H_{2,p}}{p^2} \exp(-p^2 t/\tau_{2,p}) \right]^{1/3.4} \right]^{3.4} \cos \omega t\, dt \tag{A11}$$

With the same approximation procedure as that used to derive the expression for $J_{eb}^0$ above, we obtain *approximate* expressions, namely, eq 23 for $G_b'(\omega)$ and eq 24 for $G_b''(\omega)$.

We are well aware of the fact that the approximate expressions do *not* satisfy Kramers–Kronig's relations,[64] also referred to as the generalized susceptibility. The magnitude of the errors that may arise as a result of using the approximate expressions, in lieu of exact expressions, was estimated by numerically integrating the exact expressions. We have found that the errors incurring from the use of the approximate expressions for $\eta_{0b}$, $J_{eb}^0$, $G_b'(\omega)$, and $G_b''(\omega)$ increase as the viscosity ratio of the constituent components, $\eta_{01}/\eta_{02}$, and the interaction parameter $\chi$ increase. Specifically, we have found that for the PMMA/PVDF blend system considered above the errors for $\eta_{0b}$ and $J_{eb}^0$ are about 12%, and the errors for $G_b'(\omega)$ and $G_b''(\omega)$ are about 10% and 8%, respectively, at 200 °C, but the errors become less than 2% at 230 °C.

**Registry No.** PMMA, 9011-14-7; PVDF, 24937-79-9; PSAN, 9003-54-7.

## References and Notes


(1) Han, C. D. *Multiphase Flow in Polymer Processing*; Academic Press: New York, 1981; Chapter 4.
(2) Ninomiya, K.; Ferry, J. D. *J. Colloid Sci.* **1963**, *18*, 421.
(3) Bogue, D. C.; Masuda, T.; Einaga, Y.; Onogi, S. *Polym. J. (Tokyo)* **1970**, *1*, 563.
(4) Prest, W. M.; Porter, R. S. *Polym. J. (Tokyo)* **1973**, *4*, 154.
(5) Friedman, E. M.; Porter, R. S. *Trans. Soc. Rheol.* **1975**, *19*, 493.
(6) Montfort, J. P.; Marin, G.; Arman, J.; Monge, Ph. *Polymer* **1978**, *19*, 277.
(7) Graessley, W. W. *J. Chem. Phys.* **1971**, *54*, 5143.
(8) Watanabe, H.; Kotaka, T. *Macromolecules* **1984**, *17*, 2316.
(9) Watanabe, H.; Sakamoto, T.; Kotaka, T. *Macromolecules* **1985**, *18*, 1008, 1436.

(10) Montfort, J. P.; Marin, G.; Monge, Ph. *Macromolecules* **1986**, *19*, 393, 1979.
(11) Graessley, W. W.; Struglinski, M. J. *Macromolecules* **1986**, *19*, 1754.
(12) Prest, W. M.; Porter, R. S. *J. Polym. Sci., Polym. Phys. Ed.* **1972**, *10*, 1639.
(13) Chuang, H. K.; Han, C. D. *J. Appl. Polym. Sci.* **1984**, *29*, 2205.
(14) Aoki, Y. *Polym. J. (Tokyo)* **1984**, *16*, 431.
(15) Han, C. D.; Yang, H. H. *J. Appl. Polym. Sci.* **1987**, *33*, 1199.
(16) Martuscelli, E.; Vicini, L.; Sever, A. *Makromol. Chem.* **1987**, *188*, 607.
(17) Krause, S. In *Polymer Blends*; Paul, D. R., Newman, S., Eds.; Academic Press: New York, 1978; Chapter 2.
(18) Olabisi, O.; Robeson, L. M.; Shaw, M. T. *Polymer-Polymer Miscibility*; Academic Press: New York, 1979; Chapter 5.
(19) Weeks, N. E.; Karasz, F. E.; MacKnight, W. J. *J. Appl. Phys.* **1977**, *48*, 4068.
(20) Fried, J. R.; Karasz, F. E.; MacKnight, W. J. *Macromolecules* **1978**, *11*, 150.
(21) Wignall, C. D.; Child, H. R.; Li-Aravena, F. *Polymer* **1980**, *17*, 640.
(22) Kambour, R. P.; Bopp, R. C.; Maconnachie, A.; MacKnight, W. J. *Polymer* **1980**, *21*, 133.
(23) Stejskal, E. O.; Schaefer, J.; Sefcik, M. D.; McKay, R. A. *Macromolecules* **1981**, *14*, 276.
(24) Additional data at 190 and 200 °C have been taken, after the publication of ref 13 in 1984.
(25) Wu, S. *J. Polym. Sci., Part B: Polym. Phys.* **1987**, *25*, 557.
(26) Noland, J. S.; Hsu, H. H. C.; Saxon, R.; Schmitt, J. M. In *Multicomponent Polymer Systems*; Platzer, N. A. J., Ed.; Advances in Chemistry 99; American Chemical Society: Washington, DC, 1971; p 99.
(27) Paul, D. R.; Altamirano, J. O. In *Copolymers, Polyblends and Composites*; Platzer, N. A. J., Ed.; Advances in Chemistry 142; American Chemical Society: Washington, DC, 1975; p 371.
(28) Nishi, T.; Wang, T. T. *Macromolecules* **1975**, *8*, 909.
(29) Kwei, T. K.; Frisch, H. L.; Radigan, W.; Vogel, S. *Macromolecules* **1977**, *10*, 157.
(30) Wang, T. T.; Nishi, T. *Macromolecules* **1977**, *10*, 142.
(31) This has been possible because, while presenting master curves of the dynamic storage modulus $G'(\omega)$ and dynamic loss modulus $G''(\omega)$ versus $\omega a_T$, Aoki reported the numerical values of the parameters that were used to calculate values of a temperature shift factor $a_T$.
(32) Hall, W. J.; Kruse, R. L.; Mendelson, R. A.; Trementozzi, Q. A. *Org. Coat. Appl. Polym. Sci. Proc.* **1982**, *47*, 298.
(33) Paul, D. R.; Barlow, J. W. *Polymer* **1984**, *25*, 487.
(34) Shiomo, T.; Karasz, F. E.; MacKnight, W. J. *Macromolecules* **1986**, *19*, 2274.
(35) McMaster, L. P. *Macromolecules* **1973**, *6*, 760.
(36) Seefried, C. G.; Koleske, J. V. *J. Test. Eval.* **1976**, *4*, 220.
(37) Koleske, J. V. In *Polymer Blends*; Paul, D. R., Newman, S., Eds.; Academic Press: New York, 1978; Chapter 22.
(38) Chiu, S. C.; Smith, T. G. *J. Appl. Polym. Sci.* **1984**, *29*, 1781, 1797.
(39) Han, C. D.; Yang, H. H., unpublished research, 1986.
(40) Wu, S. *Polymer* **1987**, *28*, 1144.
(41) Stein, D. J.; Jung, R. H.; Illers, K. H.; Hendus, H. *Angew. Makromol. Chem.* **1974**, *36*, 89.
(42) McMaster, L. P. In *Copolymer, Polyblends and Composites*; Platzer, N. A., Ed.; Advances in Chemistry 142, American Chemical Society, Washington, DC, 1975; p 43.
(43) Kruse, W. A.; Kirste, R. G.; Haas, J.; Schmitt, B. J.; Stein, D. J. *Makromol. Chem.* **1976**, *177*, 1145.
(44) Bernstein, R. E.; Cruz, C. A.; Paul, D. R.; Barlow, J. W. *Macromolecules* **1977**, *10*, 681.
(45) Naito, K.; Johnson, E. E.; Allara, K. L.; Kwei, T. K. *Macromolecules* **1978**, *11*, 1260.
(46) McBrierty, V. J.; Douglass, D. C.; Kwei, T. K. *Macromolecules* **1978**, *11*, 1265.
(47) Doi, M.; Edwards, S. F. *J. Chem. Soc., Faraday Trans. 2* **1978**, *74*, 1789, 1802, 1818.
(48) Graessley, W. W. *Adv. Polym. Sci.* **1982**, *47*, 67.
(49) Han, C. D.; Yang, H. H., unpublished research, 1987.
(50) Wendorff, J. H. *J. Polym. Sci., Polym. Lett. Ed.* **1980**, *18*, 439.
(51) Schmitt, B. J.; Kirste, R. G.; Jelenic, J. *Makromol. Chem.* **1980**, *181*, 1655.
(52) Han, C. D.; Lem, K. W. *Polym. Eng. Rev.* **1983**, *2*, 135.
(53) Han, C. D.; Chuang, H. K. *J. Appl. Polym. Sci.* **1985**, *30*, 2431.
(54) Han, C. D.; Ma, Y. J.; Chu, S. G. *J. Appl. Polym. Sci.* **1986**, *32*, 5597.
(55) Han, C. D.; Jhon, M. S. *J. Appl. Polym. Sci.* **1986**, *32*, 3809.
(56) Han, C. D. *J. Appl. Polym. Sci.* **1988**, *35*, 167.
(57) The Doi–Edwards tube model was used for only a single relaxation time (i.e., $p = 1$) in ref 55, but eq 27 is valid for all odd values of $p$.
(58) Han, C. D.; Kim, J. K., unpublished research, 1987.
(59) Ferry, J. D. *Viscoelastic Properties of Polymers*, 3rd ed., Wiley: New York, 1980.
(60) Struglinski, M. J.; Graessley, W. W. *Macromolecules* **1985**, *18*, 2630.
(61) Masuda, T.; Kitagawa, K.; Onogi, S. *Polym. J. (Tokyo)* **1970**, *1*, 418.
(62) Graessley, W. W. *Adv. Polym. Sci.* **1974**, *16*, 1.
(63) Doi, M.; Edwards, S. F. *The Theory of Polymer Dynamics*; Clarendon Press: Oxford, 1986.
(64) Lifshitz, E. M.; Pitaevskii, L. P. *Statistical Physics*, 3rd ed.; Pergamon Press: Oxford, 1980; Part 1, p 377.

# Characterization and Optical Anisotropy of Oligo- and Polystyrenes in Dilute Solutions

**Toshiki Konishi, Takenao Yoshizaki, Jiro Shimada, and Hiromi Yamakawa***

*Department of Polymer Chemistry, Kyoto University, Kyoto 606, Japan.*
*Received July 20, 1988; Revised Manuscript Received September 19, 1988*

ABSTRACT: Mean-square optical anisotropies $\langle\Gamma^2\rangle$ were determined from anisotropic light scattering for atactic polystyrenes of narrow molecular weight distributions in cyclohexane at 34.5 °C and in carbon tetrachloride at 25 °C over a wide range of molecular weight, including the oligomer region. No appreciable differences were observed between the results for $\langle\Gamma^2\rangle$ in the two solvents. A preliminary consideration on the basis of the rotational isomeric state model for atactic polystyrene showed that $\langle\Gamma^2\rangle$ appreciably depends on the stereochemical composition. Thus the fractions of racemic dyads $f_r$ in the samples were determined by $^{13}C$ NMR prior to the measurements and were found to be almost the same, ca. 0.59. From an analysis of the experimental data for $\langle\Gamma^2\rangle$ on the basis of the helical wormlike chain, its model parameters, i.e., the constant differential-geometrical curvature $\kappa_0$ and torsion $\tau_0$ of the regular helix that its chain contour takes at the minimum of its potential energy, the stiffness parameter $\lambda^{-1}$, and the shift factor $M_L$ (molecular weight per unit contour length), were determined for the atactic polystyrene of $f_r = 0.59$ as $\lambda^{-1}\kappa_0 = 3.0$, $\lambda^{-1}\tau_0 = 6.0$, $\lambda^{-1} = 22.7$ Å, and $M_L = 37.1$ Å$^{-1}$. Theoretical values of $\langle\Gamma^2\rangle$ calculated with these parameters well reproduced the data for $\langle\Gamma^2\rangle$ for $x \geq 5$ with $x$ the degree of polymerization of the sample. The values of $\langle\Gamma^2\rangle$ calculated for the rotational isomeric state model coincided with the experimental results for $x \leq 4$ but deviated somewhat upward for $x > 5$.

## I. Introduction

As far as the global properties of long flexible polymers are concerned, the Gaussian chain model provides a good theoretical basis for calculations of their dilute solution properties.[1] However, a more precise polymer model reflecting the details of the chain structure is needed to

0024-9297/89/2222-1921$01.50/0 